

Article

Comparative Studies on Sorption Recovery and Molecular Selectivity of Bondesil PPL versus Bond Elut PPL Sorbents with Regard to Fulvic Acids

Anna N. Khreptugova, Tatiana A. Mikhnevich, Alexandra A. Molodykh, Sofia V. Melnikova, Andrey I. Konstantinov, Gleb D. Rukhovich, Alexander B. Volikov  and Irina V. Perminova * 

Department of Chemistry, Lomonosov Moscow State University, Leninskie Gory 1-3, 119991 Moscow, Russia; khreptugova@mail.ru (A.N.K.); tanya.4erkasova8q@gmail.com (T.A.M.); alex-molod@yandex.ru (A.A.M.); sonyamelnikova20@gmail.com (S.V.M.); noogen@inbox.ru (A.I.K.); rukhovich@gmail.com (G.D.R.); ab.volikov@gmail.com (A.B.V.)

* Correspondence: iperm@med.chem.msu.ru

Abstract: Large scale isolation—in gram quantities—of dissolved organic matter (DOM) from natural waters is necessary for detailed investigation of its role in chemical and microbial processes driving carbon cycling under conditions of global climate change. The best candidate for a use in these large-scale experiments is a bulk sorbent Bondesil PPL, which has the same modification as the widely used Bond Elut PPL sorbent. There have been no studies so far reported on interchangeability of these sorbents with regard to DOM isolation. This work was devoted to comparative studies on sorption efficiency and molecular selectivity of these two sorbents—Bond Elut PPL and Bondesil PPL with regard to DOM components. Fulvic acids (FA) from peat water leachate were used as a model DOM. Laboratory solid phase extraction (SPE) setup was used for monitoring sorption recovery and extraction yield. It included three parallel experiments on pre-packed Bond Elut PPL cartridges (500 mg/3 mL) and three self-packed Bondesil PPL cartridges (500 mg/3 mL). Fourier transform ion cyclotron resonance mass spectrometry (FT ICR MS) and $^{13}\text{C}/^1\text{H}$ nuclear magnetic resonance (NMR) spectroscopy were used for determination of molecular and structural group compositions of the FA isolates obtained with a use of two different sorbents. The results of this study allowed a conclusion on interchangeability of the two sorbents used in this study for the purposes of DOM isolation from natural waters. This conclusion was backed up by similarity of sorption behavior of the peat FA components on both sorbents and by high similarity of molecular compositions and carbon distribution among the main structural groups.

Keywords: dissolved organic matter (DOM); fulvic acids; solid phase extraction; large scale isolation; Bond Elut PPL; Bondesil PPL; FT ICR MS; NMR; molecular composition; sorption selectivity



Citation: Khreptugova, A.N.; Mikhnevich, T.A.; Molodykh, A.A.; Melnikova, S.V.; Konstantinov, A.I.; Rukhovich, G.D.; Volikov, A.B.; Perminova, I.V. Comparative Studies on Sorption Recovery and Molecular Selectivity of Bondesil PPL versus Bond Elut PPL Sorbents with Regard to Fulvic Acids. *Water* **2021**, *13*, 3553. <https://doi.org/10.3390/w13243553>

Academic Editor: Cidália Botelho

Received: 25 November 2021

Accepted: 10 December 2021

Published: 12 December 2021

Publisher's Note: MDPI stays neutral with regard to jurisdictional claims in published maps and institutional affiliations.



Copyright: © 2021 by the authors. Licensee MDPI, Basel, Switzerland. This article is an open access article distributed under the terms and conditions of the Creative Commons Attribution (CC BY) license (<https://creativecommons.org/licenses/by/4.0/>).

1. Introduction

Dissolved organic matter (DOM) significantly influences photoinduced, chemical, microbial, and geochemical processes, which take place in natural waters. These processes include complexation with heavy metals and microelements, electron transfers, solubilization of pesticides and hydrocarbons, electron shuttling within microbial communities, and others [1–3]. DOM represents a global reservoir of organic carbon. Information on molecular composition of DOM is indispensable for understanding its role in chemical and microbial processes driving carbon cycling under conditions of global climate change [4,5]. Large scale isolation—in gram quantities—of dissolved organic matter (DOM) from sea waters is necessary for detailed investigation of relationships between molecular compositions and functions of DOM in marine environments. This step is necessary due to extremely low content of dissolved organic carbon (DOC) in the sea water varying from 0.1 to 5 g/L and high content of salts [6].

There are several methods of DOM isolation from aquatic systems including sorption onto Amberlite resins (e.g., XAD-8, XAD-4) recommended by International Humic Substances Society (IHSS) as a standard procedure [7–9], reverse osmosis/electrodialysis [10,11], and solid phase extraction (SPE) using prepacked cartridges [11–14]. Currently, the most widely accepted method of DOM isolation is SPE [15]. Its major advantage over the resin extraction is a use of methanol for elution of the sorbed DOM, which enables for skipping desalting of the DOM extract—obligatory step in XAD-resin isolation protocol [7]. The best efficiency of SPE cartridges was achieved for Bond Elut PPL and reached up to 60–70% [12,16], which is higher than the corresponding values for XAD-8 resin (up to 40–50%) [9]. The Bond Elut PPL represents a modified co-polymer of polystyrene and divinylbenzene, which was created for sorption of phenols, and performs particularly well under conditions of high content of salts typical of marine waters [6,12]. Application of Bond Elut PPL cartridges for isolation of the Suwannee River DOM gave DOC recovery results of 89% [16]. Comparison of three types of sorbents (C-18, PPL, and HLB) was reported for DOM and lignin-phenols [17]. It showed that DOC recovery was the best for PPL (60% for rivers and 47% for coastal DOM). Rapid SPE technique developed for DOM isolation showed the maximum DOC recovery of 78% [13].

Along with the clear advantages, a use of the prepacked cartridges (e.g., Bond Elut PPL) has substantial limitations for the DOM isolation due to limited sorption capacity. This is because the largest prepacked cartridges contain only 5 g of sorbent per 60 mL tube (Bond Elut PPL MegaPack, Agilent Technologies, USA). At the same time, for large scale filtration aimed to isolate gram quantities of DOM, much bigger amounts of sorbent are needed. The regular approach for solving this problem is to use bulk sorbent for packing custom-size column or cartridges. However, Agilent Technologies does not provide Bond Elut PPL as a bulk sorbent. Instead, the company's catalogue offers Bondesil PPL sorbent. There is no information provided what kind of polymeric base has this sorbent. The safety data sheet only reports that it is 100% polymeric. The producer catalogue provides the info on the bead size of 125 μm , the pore size of 150 \AA , specific area of 600 $\text{m}^2 \cdot \text{g}^{-1}$. The large surface area promises good sorption characteristics, whereas large pore size is preferential for high desorption recovery. Still, there are no reports available on either performance assessment of Bondesil PPL versus Bond Elut PPL with regard to isolation of DOM, or on the comparison of the quality of the SPE-DOM isolated with a use of those two sorbents. The latter problem is of extreme importance due to complexity of molecular composition of DOM, which is widely used as an indicator and predictor of the global environmental processes, e.g., inflow of terrestrial DOC into marine environments, mapping the origin of river plumes. In this case a change in molecular composition of the DOM isolate, which was brought about by a purely methodical bias (molecular selectivity of the new sorbent) can lead to erroneous conclusions and interpretations with regard to the course of environmental processes. The existence of molecular selectivity is numerous reported [17,18]. Our previous studies have shown [18] that a use of Bond ELut PPL cartridges versus Amberlite XAD-8 resin gave very different samples of DOM from the same water: the former were enriched with aliphatic components, whereas the latter were rich in aromatic structures. This is why it is very important to exclude methodological bias from interpretation of geochemical and environmental processes which are based on the molecular composition of NOM.

The aim of this work was to assess sorption properties of Bondesil PPL with regard to DOM, to compare extraction performance of self-packed Bondesil PPL cartridges versus prepacked Bond Elut PPL cartridges, and to compare molecular composition and structural characteristics of the obtained isolates using Fourier Transform Ion Cyclotron Resonance Mass Spectrometry (FT ICR MS) and NMR spectroscopy. FT ICR MS technique has been proven extremely useful for characterization of specific molecular features of DOM from different sources [19–24]. Another powerful technique for structural characterization of HS and DOM is NMR spectroscopy [25–28], and particular advantages were achieved with a combined use of FT ICR MS and NMR analyses [studies of DOM] a combined use of

FT ICR MS and NMR spectroscopy [29–32]. This motivated us for a use of both FT ICR MS and NMR techniques for achieving the unambiguous results on characterization of potential molecular selectivity of the SPE sorbents used in this study.

2. Materials and Methods

2.1. Materials

Commercially available sample of fulvic acids (FA) under the trade name “FulvAgra” was provided by Humintech Ltd. (Grevenbroich, Germany). The source of this commercial FA is water leachate of underground peat deposit. It was used without further purification. High grade purity HCl (Chimmed, Russia) was used for acidification. High-purity deionized water was prepared from feed distilled water using a Milli-Q Simplicity 185 water purifying system (Merck, Darmstadt, Germany). HPLC grade methanol (JT Baker, Avantor, Radnor, PA, USA) was used for elution of the sorbed FA from the cartridges. Hypergrade methanol (for LC-MS LiChrosolv, Merck, Darmstadt, Germany) was used for DOM elution and samples dilution for FT ICR MS analysis. The SPE cartridges were Bond Elut PPL (500 mg per 3 mL) (Agilent Technologies, Waldbronn, Germany). The bulk sorbent was Bondesil PPL (Agilent Technologies, Waldbronn, Germany). The empty cartridges (3 mL tubes) were purchased from Agilent Technologies, Waldbronn, Germany).

2.2. TOC Measurements

Concentrations of the initial FA solutions and permeates were determined according to [33] using a high temperature combustion total organic carbon analyzer (TOC-L CSN, Shimadzu, Japan). For this purpose, aliquotic parts of permeates and eluates (500 μ L and 100 μ L, respectively) were evaporated and redissolved in 1 mL of MiliQ water for analysis. After every 5 DOC measurements, the measurements of a blank sample with MiliQ water and a standard solution of potassium phthalate were performed. The data were blank corrected and standard deviations between replicate sample injections ($n = 3$) were calculated.

2.3. SPE Extraction Protocol

The SPE extraction was performed with a use of a vacuum manifold (Phenomenex, Torrance, CA, USA) equipped with a vacuum pump Portlab N86KTE 18 (Knauer, Berlin, Germany). Six volumes of feed FA solution (6×2 L) were prepared at a concentration of 50 mg/L by dissolving a weight of dry FA sample (0.1 g) in 2 L of Milli-Q water. Prior to extraction, the FA solutions were acidified until pH 2 by using 20% HCl and degassed using vacuum pump. Three SPE cartridges were packed with a 0.5 g weight of Bondesil PPL sorbent each by placing a weight into a 3 mL empty SPE tube. Three prepacked Bond Elut PPL cartridges were used for extraction of FA. The prepared cartridges were used for three parallel extraction experiments which included a use of one prepacked cartridge Bond Elut PPL and one cartridge self-packed with Bondesil PPL. The two cartridges were mounted into a vacuum manifold equipped with a vacuum pump. The extraction protocol followed the method described by Dittmar et al. [12]. It included preconditioning of the SPE sorbent with a use of one cartridge volume of MeOH followed by two volumes of water acidified to pH 2. A 2 L sample of FA was discharged through each preconditioned cartridge by 500 mL portions at the rate of 15–20 mL/min using a vacuum pump. The solution at the exit of cartridge was collected into the glass vessel for absorption measurements, which is necessary for sorption efficiency determination. The measurements were made after passage of each 500 mL portion. After discharge of all four 500 mL volumes of the FA solution, the loaded SPE cartridge was desalted by passing two cartridge volumes of acidified water at pH 2 and dried thoroughly with air flow. DOM elution was conducted with a use of 8 mL of methanol. The DOM eluates in methanol were rotor-evaporated, redissolved in Milli-Q water and lyophilized using a freeze drier Scientz-18ND Top Press multi-manifolds (Scientz, Ningbo, Zhejiang, China). The round-bottom glass flasks were used for lyophilization. They were combusted prior to use for 4 h at 450 °C. The dry

samples were transferred into a glass screwed vial and kept in refrigerator at 4 °C in the dark.

2.4. Determination of Sorption and Extraction Efficiencies for DOM Isolation

The sorption efficiency of both sorbents was estimated using UV-Vis measurements (the absorbance at 254 nm) of FA solutions before and after they passed through the sorbents. The concentration of FA was calculated using calibration curve plotted from the values of optical density (OD) measured at 254 nm at FA concentrations of 1, 5, 10, 20, 25, 50 mg/L at pH 2. The calibration solutions were prepared by appropriate dilutions of the FA stock solution of 100 mg/L (0.01 g of FA per 100 mL of acidified water at pH 2). The equation of calibration curve was linear with a slope of 0.0137 L/mg FA. The amount of the sorbed FA was calculated as a difference between the initial and exited concentrations of the FA solutions multiplied with a 2 L volume of discharged FA. It was divided with a weight of the dissolved FA (0.1 g) and expressed in percentage using the following equation:

$$R = \frac{\text{DOC}_{\text{ext}}}{\text{DOC}_{\text{init}}} \times 100\%, \quad (1)$$

where R is the sorption recovery, DOC_{ext} is a weight of the FA extracted by the sorbent and DOC_{init} stands for the weight of the discharged FA. The elution of DOM from the loaded cartridge was conducted after desalting and thorough drying of the cartridge. The extraction efficiency was calculated as a ratio of the eluted to the discharged mass of FA. The eluted mass was determined gravimetrically. The discharged mass was calculated from initial concentration of the FA solution and its discharged volume.

2.5. UV-Vis Measurements

UV-Vis measurements were carried out using a Carry 400 Probe spectrophotometer (Varian, Palo Alta, CA, USA) in the range from 200 to 500 nm in a 1 cm quartz cell. Specific ultraviolet absorbance (SUVA₂₅₄) was calculated as a ratio of the OD value at 254 nm to a concentration of total organic carbon [17,18]. All measurements were conducted in triplicate.

2.6. NMR Analysis

Quantitative ¹H and ¹³C solution state NMR spectra were acquired using Avance-400 spectrometer (Bruker BioSpin, Ettlingen, Germany) operating at 400 MHz proton frequency on the samples dissolved in 99.9% D₂O at a concentration of 45 mg/mL. The conditions for quantitative measurements of carbon distribution were set as described in [34,35]. To exclude the Nuclear Overhauser effect while recording ¹³C NMR spectra, the pulse technique INVGATE was used. For complete carbon nuclei relaxation, pulse delay for ¹³C NMR spectra recording was set to 8 s, the number of scans averaged was 4500. All NMR spectra were acquired after centrifugation using a 5-mm broadband probe.

2.7. FT ICR MS Analysis and Data Treatment

Ultrahigh-resolution mass spectra were acquired on a Bruker solariX 15 T FT ICR mass spectrometer (Bruker Daltonics, Bremen, Germany) equipped with a 15 Tesla superconducting magnet and an Apollo II source located at the user facilities of the Zelinski Institute of Organic Chemistry of RAS. The acquisition conditions applied in this study followed those described in [31]. The samples were injected with a constant flow rate of 120 μL/h, nebulizer gas pressure of 2.2 bar, and drying gas pressure of 4 bar at 200 °C. Accumulation time was 0.4 sec. The ESI voltages were 3600 V for the capillary voltage and −500 V (the end plate offset). The spectra were acquired using a time transient of 4 MW. MS parameters were optimized to reach a maximum of sensitivity in the m/z range of 150–1000. The resulting transfer optic parameters were ToF 0.6 msec, frequency 4 MHz, and RF amplitude of 175 V. In this case, 300 scans were acquired for each sample.

The molecular formulae assignments were made using lab-made Transhumus software developed by Anton Grigoriev. The mass accuracy window was set at a value of <0.5 ppm (Da/MDa), and the chemical constraints were used as described in [36], nominally: the value of O/C ratio was ≤ 1 , the value of H/C laid between 0.3 and 2.2, the amount of C atoms topped 120, the amount of H atoms topped 200, the amount of O atoms laid between 1 and 60, the amount of N atoms was 0 or 1. The acquired mass list was recalibrated using unambiguous identifications and total mass difference statistics (TMDS) analysis [37]. The obtained molecular assignments were used for calculation of H/C and O/C ratios, which were plotted as Van Krevelen diagrams represented by a relationship of H/C versus O/C values as described by Kim et al. [38].

Similarity assessment of molecular compositions assigned to mass lists of all SPE isolates under study was conducted in accordance with the statistical procedures described in [39]. Firstly, the Jaccard similarity indices (J index) were calculated for each pair of samples [40,41]. The J index can be formally defined as an amount of formulae in the intersection of two sets of formulae related to the total number of formulae in the two samples. The mathematical representation of the J index for the two samples (1 and 2) is written as:

$$J(A, B) = \frac{|A \cap B|}{|A \cup B|} = \frac{|A \cap B|}{|A| + |B| - |A \cap B|}, \quad (2)$$

where A and B are the sets of the formulae assigned to the samples 1 and 2, respectively, the numerator is the number of common formulae in the molecular composition of the samples 1 and 2, and the denominator is the total number of formulae assigned to the samples 1 and 2.

For correlation analysis, the quantitative treatment of the Van Krevelen diagrams was conducted using a cell-partitioning algorithm as described by Perminova [42]. It implies binning of the Van Krevelen diagram area into 20 cells followed by calculation of population distribution based on occupational densities. For this purpose, the intensity-weighted occupational density was calculated for each cell (D_k) using the following equation:

$$D_k = \frac{\sum_{i=1}^{N_k} I_i}{\sum_{j=1}^N I_j}, \quad k = 1, 2, \dots, n \quad (3)$$

where D_k is the intensity weighted occupational density of the cell k ($k = 1 \dots n$), I_i is the peak intensity in mass list assigned with this specific formula (N_k formula), and I_j is the sum intensity of all peaks with assigned formulae (N formulae).

The obtained values of occupational densities comprised 20-dimensional vectors (D_1 – D_{20}), which were further used as quantitative descriptors of the molecular composition. The squared values of correlation coefficients between all pairs of vectors were calculated and used as a measure of the similarity of the samples (Cell Correlation). J indices and cell correlations for all pairs of the FA Bond Eut and FA Bondesil isolates were plotted in similarity heatmaps. For the three sets of samples (FA_BE, FA_BS, FA_initial), average values and standard deviations were calculated for the occupational densities (D_1 – D_{20}). The average values and standard deviations were displayed on bar plots distributed on the van Krevelen diagram in accordance with the location of the corresponding cells (1–20). The mapping of Van Krevelen diagram with regard to the eight chemotypes was according to [42,43].

3. Results and Discussion

3.1. Comparison of Sorption Recoveries of the Bond Elut PPL and Bondesil PPL Sorbents

The main question of this study was whether Bond Elut PPL (BE) and Bondesil PPL (BS) sorbents could be considered as interchangeable ones with regard to SPE extraction of DOM from natural waters. For answering this question, we had to compare, first of all, the extensive parameters characteristic to quantity of the isolated sample, such as sorption and elution recoveries with regard to the FA sample used in this study. Secondly,

we had to compare “intensive parameters” such as similarity of molecular composition of the isolates extracted with different sorbents and their similarity to the parent DOM. The results of comparative studies on the sorption recoveries of BE- and BS-sorbents are shown in Figure 1. It shows the values of sorption recovery of both sorbents at the growing loadings of the sorbent with DOM in the form of the FA sample used in this study. Each data point corresponds to the value of sorption efficiency after passage of each 500 mL portion of FA solution through the cartridge.

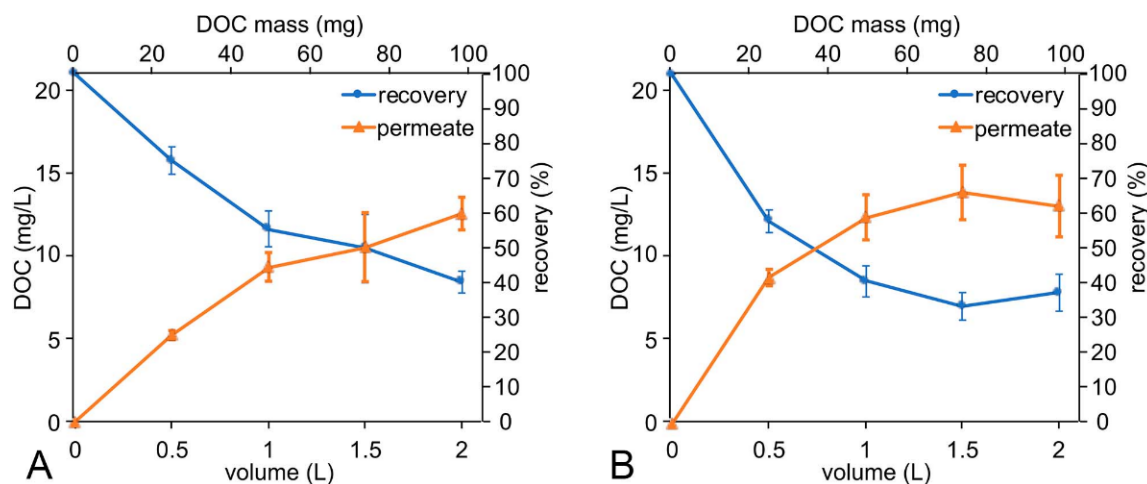


Figure 1. Mean values and sorption recoveries of dissolved organic carbon (DOC) with standard deviation ($n = 3$) from 50 mg/L FA solution: (A) for the pre-packed (500 mg per 3 mL) Bond Elut PPL cartridges (experiment was run in triplicate); and (B) for the self-packed (500 mg per 3 mL) Bondesil PPL cartridges (experiment was run in triplicates). FA solution was discharged at a flow rate of 20 mL/min. DOC (mg/L) concentrations of permeates are shown on the left y -axis, the DOC recovery is demonstrated on the right y -axes.

Figure 1 demonstrates the dependence of DOC concentration (mg/L) in permeate and of the sorption recovery (%) of sorbents on the discharged volume of the FA solution, which is proportional to the loading of the sorbent. The maximum sorption recoveries for both BE- and BS-sorbents were reached at the minimum loading—after the passage of the first 500 mL portion of the 50 mg/L FA solution (the loading equaled to 12.5 mg FA or 5 mg DOC per 500 mg of sorbent). The maximum sorption recovery values were $(75 \pm 4)\%$ and $(58 \pm 3)\%$ for Bond Elut PPL and Bondesil PPL, respectively. Hence, the value of sorption recovery of Bond Elut PPL was about 15% higher as compared to the corresponding value for the Bondesil PPL. After the second portion of FA, the sorption recoveries dropped down substantially—down to 55% for Bond Elut PPL, and much more—down to 40%—for Bondesil PPL. After the third and fourth portions, the sorption recovery for Bond Elut PPL continued to decrease gradually down to 50%, and then—to 40%, respectively. At the same time there was no further drop observed in sorption recovery of Bondesil PPL: it leveled off at the value of 40%. As a result, after passage of the final—fourth portion of the FA solution, which corresponded to the loading of 100 mg FA (or 40 mg DOC) per 500 mg of the sorbent, the sorption recovery of the both sorbents became comparable and accounted for $(40 \pm 3)\%$ and $(38 \pm 3)\%$ for the Bond Elut PPL and for the Bondesil PPL, respectively.

The obtained data are very similar to the trends reported in [16] where an impact of the DOM loading was studied on sorption recovery of Bond Elut PPL cartridges. Same as in our studies, the authors observed the similar trends, which differ substantially from the classical breakthrough curve: it should be independent on the loading [44]. For explanation of the experimental data, Li et al. [16] suggested that the least strongly absorbed DOM molecules were substituted with more aromatic and aliphatic compounds under overloading of the sorbent. This phenomenon could explain non-classical character of the breakthrough curve of DOM on the Bond Elut PPL sorbent. Thus, the cartridge loading consists only 40% of initial FA concentration. The differences in DOC recovery were also demonstrated in [13],

where the recovery value R ranged from 31% to 57% depending on the DOM source, its composition and structure. The authors considered overloading as one of the main factors which influenced the sorption recovery of DOM.

For determination of extraction recovery, the dry isolated DOM samples were weighted and the obtained value was divided with the weight of the discharged FA and expressed in percentage. Unfortunately, two glass flasks with the Bondesil PPL isolates cracked in a freeze dryer, we could not assess the yield quantitatively for the samples FA-Bondesil 2 and FA_Bondesil 3. As a result, the needed estimate was obtained only for FA_Bondesil_1. The data on extraction recovery of the sorbents used in this study are shown in Figure 2 and highlighted in colors.

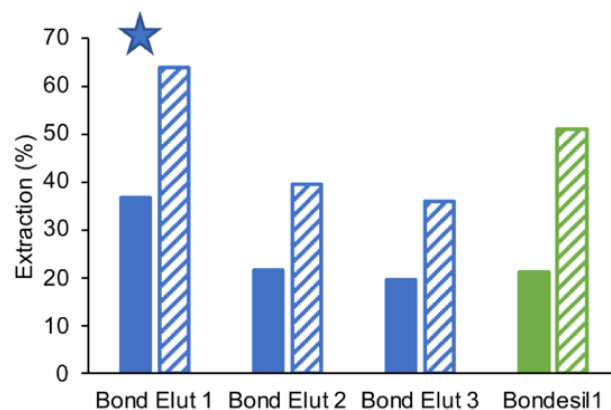


Figure 2. Extraction efficiency of Bond Elut PPL ($n = 3$) and the Bondesil PPL after passage of 100 mg FA (2 L of 50 mg/L FA solution) per 500 mg sorbents. One Bond Elut PPL cartridge was characterized with higher-than-average results—it is marked with a star. The solid columns refer to the extraction efficiency values normalized to the total amount of the discharged FA (100 mg). The striped columns refer to the extraction efficiency values normalized to the real loading of sorbents.

Figure 2 shows that for the high loading used in this study (100 mg of FA were discharged through 500 mg of the sorbet) the extraction efficiency accounted for 25% and 21% for the Bond Elut PPL cartridges and the self-packed Bondesil PPL columns, respectively. The striped histograms show the extraction efficiency normalized to the expected loading of the column (100 mg FA or 40 mg DOC per 500 mg) and the solid columns show extraction efficiency normalized to the factual amount of the sorbed FA. The average values for the “real” extraction efficiencies were 46% and 50% for Bond Elut PPL and Bondesil PPL, respectively. These low values might be indicative of the high losses of the DOM sample due to irreversible adsorption on the sorbent. In general, the obtained data show loading-dependent sorption of DOM of both sorbents used in this study. Bond Elut PPL has preferential sorption recovery with regard to DOM when low loadings are used. However, under conditions of high loading the recoveries of both sorbents become comparable. From this point of view, both sorbents could be used for DOM isolation.

3.2. FT ICR Mass Spectrometry of the Fulvic Acids (Pure and Isolated with Bond Elut PPL and Bondesil PPL Cartridges)

Along with the sorption recovery, the potential molecular selectivity of the sorbent with regard to specific components of the complex mixtures is another important issue which should be considered. The existence of this problem for DOM extraction was substantiated by our previous studies [18] as well as by other researchers [16]. This is why all SPE isolates were examined for identity of both molecular and structural group compositions using FT ICR MS and NMR spectroscopy, respectively. The obtained data were also compared to the compositional space of the parent FA. For the purpose of this study, we have acquired FT ICR MS data for three sets of samples: three BE isolates of FA (FA_BE1, FA_BE2, FA_BE3), three BS isolates of FA (FA_BS1, FA_BS2, FA_BS3), and two spectra of the parent FA (FA1 ad FA2). The FT ICR MS data were processed by assigning

molecular formulae ($C_xH_yO_zN_n$) as described in the Experimental section. The general characteristics of the FT ICR MS spectra obtained in this study are summarized in Table 1.

Table 1. An overview of the FT ICR MS data obtained for the FA isolates in this study.

	FA_BE1	FA_BE2	FA_BE3	FA_BS1	FA_BS2	FA_BS3	FA1	FA2
Formulae, total	4749	5398	4243	4308	4178	4702	5280	4509
CHO, number	4526	5217	4178	4231	4149	4475	5091	4150
CHON, number	223	181	65	77	29	227	189	359
CHO, %	95	97	98	98	99	95	96	92
CHON, %	5	3	2	2	1	5	4	8
M_n^* , Da	570	609	569	548	518	554	574	560
DBE_n	13.0	15.0	14.5	13.1	12.6	12.4	12.3	12.3
$(H/C)_n$	1.12	1.07	1.03	1.09	1.08	1.16	1.17	1.14
$(O/C)_n$	0.42	0.42	0.41	0.41	0.41	0.39	0.42	0.44

* Subscript “n” indicates number-averaged values.

All three sets of samples were characterized by similar amount of assigned formulae (4797 ± 472) for FA_BE, (4396 ± 223) for FA_BS, (4895 ± 386) for the parent FA, and by the dominant contribution of CHO compositions (95%). For the set of FA_BS samples, the lower values of the number-averaged molecular weight were observed (540 ± 16) as compared to those for the FA_BE samples (583 ± 19) and for the FA replicas (567 ± 7). Much larger variations were observed for the number-averaged values of DBE: on average, the molecular components of the FA_BE isolates were characterized with the larger DBE values both as compared to the FA_BS isolates (1.5 DBE) and the parent FA (1.9 DBE). In sync with the trend observed for the DBE values, the highest values of H/C ratio were seen for the parent FA (1.14–1.17), whereas both groups of SPE isolates were characterized with the lower H/C values: (1.03–1.12) for the FA_BE samples and (1.08–1.16) for the FA_BS samples. This trend is indicative of the more saturated character of the parent FA as compared to both types of isolates. This phenomenon can be explained by higher affinity of aromatics-enriched FA components for the sorbent material as compared to more saturated components, of particular, containing hydrophilic carbohydrates.

The values of H/C and O/C ratios calculated for all individual peaks were plotted in the corresponding Van Krevelen diagrams (Figure 3). Figure 3 shows that the Van Krevelen diagrams of the isolates derived with Bond Elut PPL and Bondesil PPL cartridges (Figure 3a–f) are very similar. They are characterized by the most densely populated area within the range of values: $0.6 < H/C < 1.4$, $0.25 < O/C < 0.75$, which are characteristic for condensed oxidized and more saturated ligninic compounds. The molecular composition of the parent FA sample (Figure 3g,h) is visually different from the SPE isolates: it is characterized by the presence of considerable amount of highly oxidized components ($O/C > 0.75$) and by the higher content of low oxidized aliphatic components ($H/C > 1.4$, $O/C < 0.25$). To quantify the similarities and differences of the obtained molecular compositions, the Jaccard similarity indices (J index, Equation (2)) were calculated for each pair of mass spectra. The results are shown as a heatmap in Figure 4.

The values of the J index for the FA_BE set of samples were in the range from 0.59 to 0.61, for the FA_BS set of samples—from 0.56 to 0.67, and for the parent FA—0.64. The obtained data are indicative of closer similarity of the FA_BS samples to one another as compared to the FA_BE samples. At the same time, the identity within the triplicates of FA isolates was less as compared to two spectra of the same sample of the parent FA, which could be expected. On average, the similarity between the FA_BE and FA_BS sets was on the same level as the internal similarity of these sample sets. The values of the J indices between the SPE samples (FA_BE and FA_BS) and the parent FA were in the range from 0.48 to 0.66, and, in general, lower as compared to the pairs from the FA_BE and FA_BS sets. It can be concluded that a use of Bond Elut PPL and Bondesil PPL cartridges yields the molecular compositions of isolates which are same identical as if the only one type of cartridges was used.

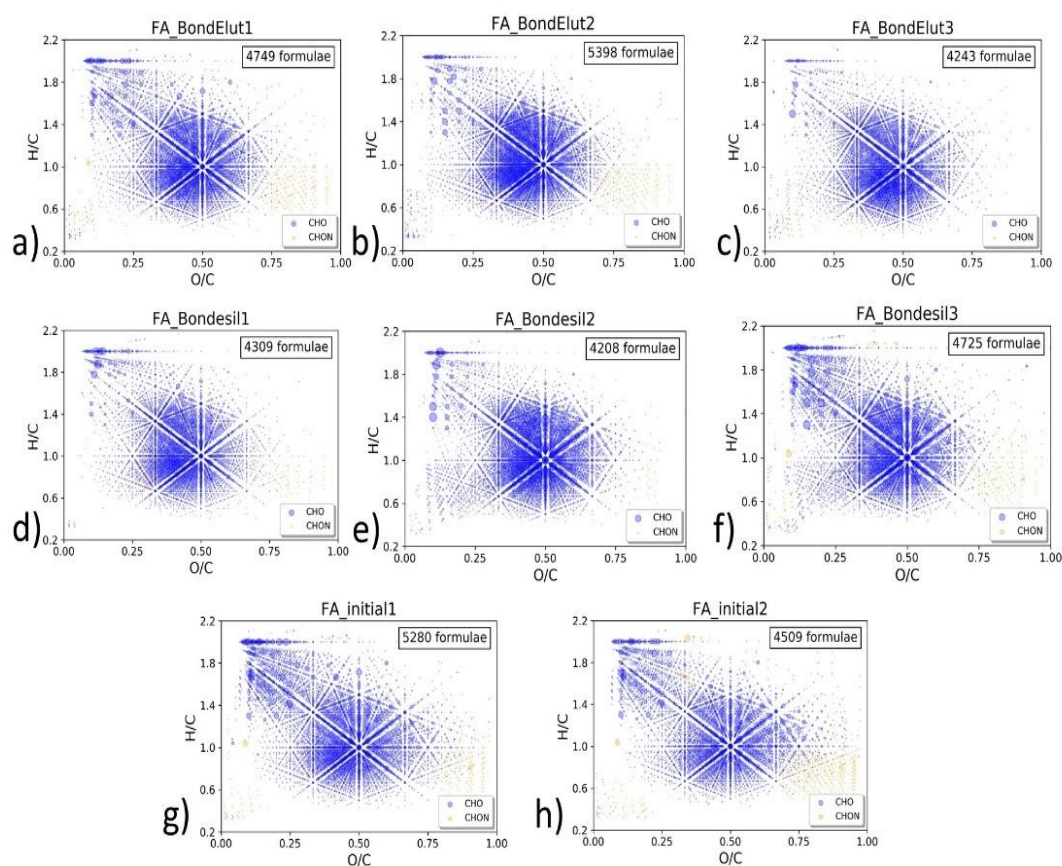


Figure 3. Van Krevelen plots for the three FA-BE samples (a–c), for the three FA_BS samples (d–f), and for the two spectra of the parent FA (g,h). The dot size corresponds to the peak intensity in the mass list. CHO formulae are highlighted in blue, and CHON—in yellow. The number of assigned formulae for the sample is displayed in the upper right corner.

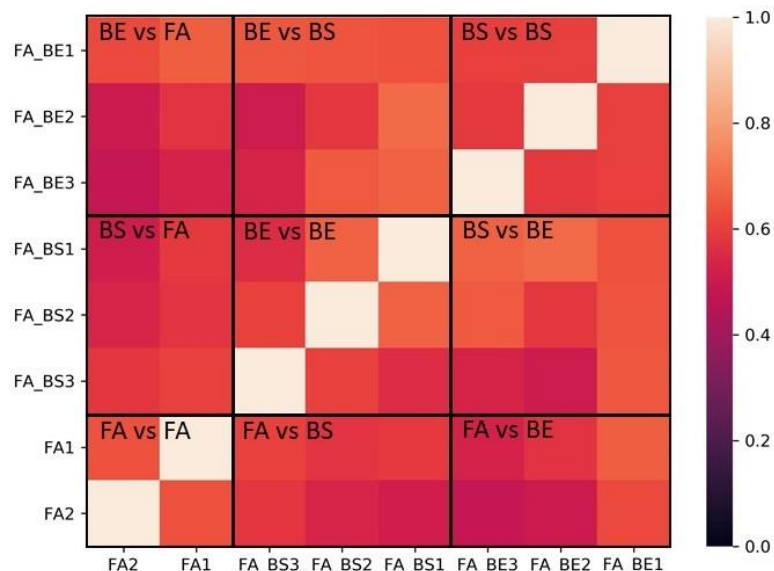


Figure 4. The heatmap from the values of J index calculated for each pair of the samples used in this study as an intersection of shared molecular formulae to the total number of formulae in the pair of samples. The color bar refers to the value of the J indices and the Cell Correlations (R^2). The heatmap is divided into blocks corresponding to the number of samples in each set: FA_BE (Bond Elut PPL, 3 samples), FA_BS (Bondesil PPL, 3 samples), and FA (2 samples).

For all pairs of the investigated samples, the value of J index did not exceed 0.69, which means that even the most similar samples shared not more than 69% of formulae found in both samples. For comparison, Mosher et al. studied molecular composition of three DOM samples from the same stream using FT ICR MS, and obtained J index values in the range from 0.74 and 0.8 [45]. The maximum value of J index of 0.57 (the best match) was reported for the interlaboratory study of molecular compositions of six HS samples with a use of five different mass spectrometers [39]. The same study demonstrated that much more robust and convincing results were obtained for similarity analysis conducted with a use of the occupation density descriptors. The corresponding descriptors can be easily calculated as described by Perminova (2019) [42] by binning the Van Krevelen diagram into 20 cells and computing occupation density of each cell with a use of Equation (3). As a result, molecular composition of each sample can be described with 20-dimensional vector (Equation (2)) defined by values of 20 occupational densities (D_1 – D_{20}) corresponding to 20 cells of the Van Krevelen diagram. In this case, the samples similarity can be judged based on a value of the determination coefficient (R^2) between each pair of vectors (Cell Correlation). The obtained results are shown in heatmap in Figure 5.

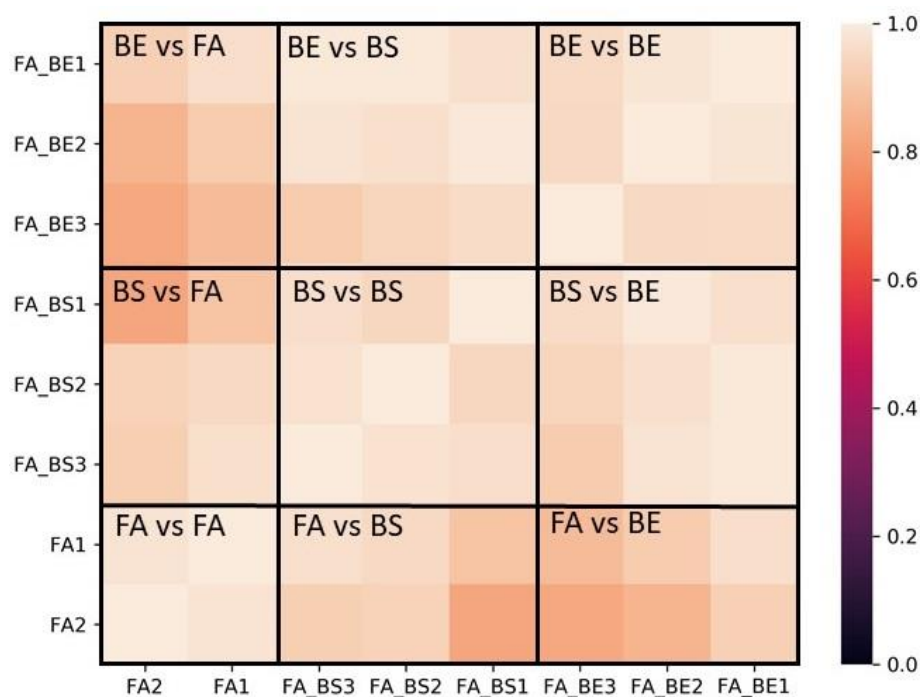


Figure 5. The heatmap for the values of Cell Correlations (R^2) calculated for each pair of the samples used in this study. The color bar refers to the value of the Cell Correlations (R^2). The heatmap is divided into blocks corresponding to the number of samples in each set: FA_BE (Bond Elut PPL, 3 samples), FA_BS (Bondesil PPL, 3 samples), and FA (2 samples).

It can be seen that a use of occupational densities resulted in much higher similarity of the samples (R^2 close to 1) as compared to the calculation of J indices. Comparison of the obtained values of internal correlations within the sets of FA_BE, FA_BS and FA and those for the pairwise correlations between the sets of FA_BS and FA_BE corroborated well the conclusions made on the basis of the J index values. Nominally, the prevailing majority of FA_BE and FA_BS pairs (7 out of 9) turned out to be as (or more) similar to each other as the samples extracted by the same type of sorbent ($R^2 \geq 0.95$), and 4 pairs—as two spectra of the same FA sample ($R^2 \geq 0.98$). In general, the SPE isolates were less similar to the parent FA than to each other ($0.82 \leq R^2 \leq 0.97$).

For better illustration of the similarities and differences in the distribution of occupational densities on the Van Krevelen diagram within the three sets used in this study, the average values and standard deviations for D_1 – D_{20} were displayed as bar plots and placed

on the Van Krevelen diagram in accordance with the location of the corresponding cells (1–20) (Figure 6).

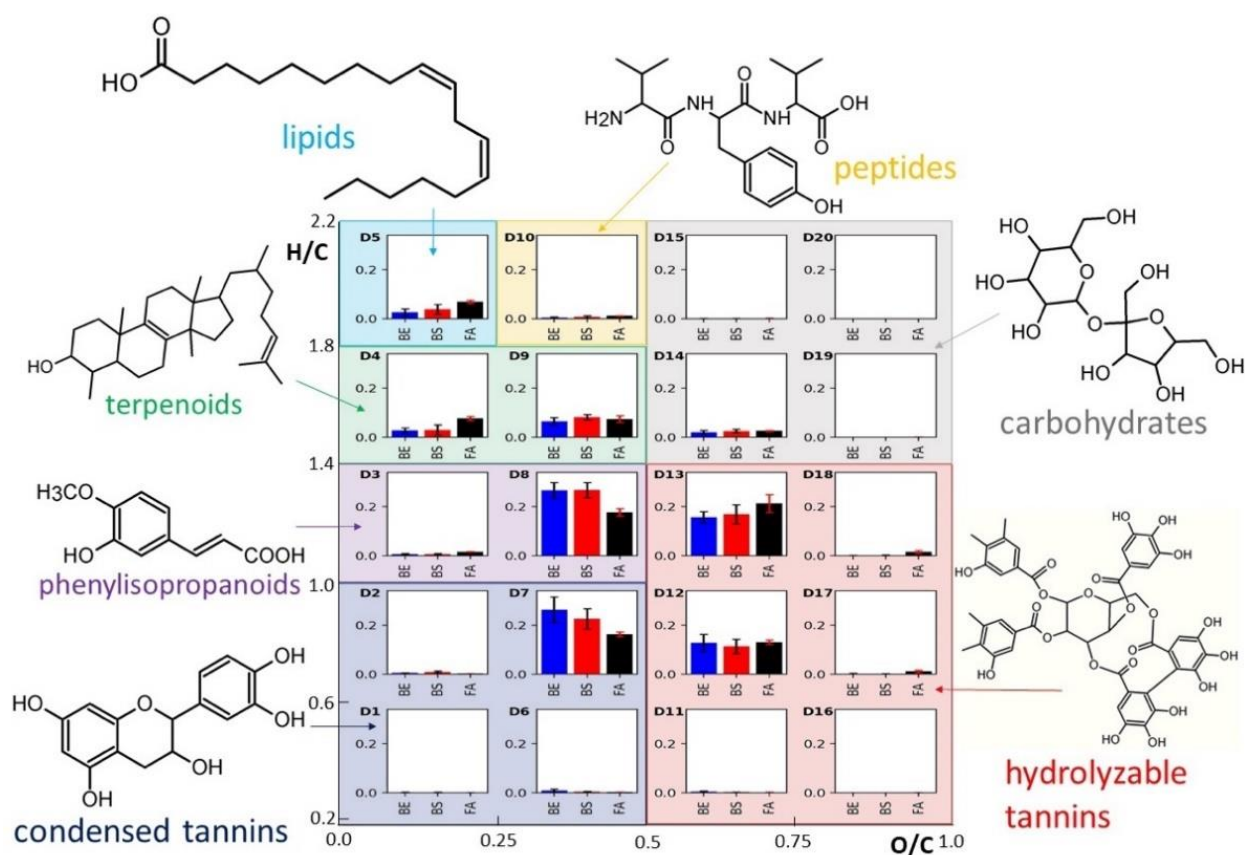


Figure 6. Mean values and standard deviations of the occupational densities of 20 cells in the split Van Krevelen diagram (D_1 – D_{20}) for FA_BE set (the columns are highlighted in blue), for FA_BS set (the columns are highlighted in red), and for the parent FA (the columns are highlighted in black). The plots are arranged in accordance to the cells' location in the Van Krevelen diagram (1–20). The background colors refer to the seven main chemotypes depicted by the chemical formulae: condensed tannins (gray), phenylisopropanoids (lignins) (lilac), terpenoids (green), lipids (turquoise), peptides (yellow), carbohydrates (light gray), hydrolysable tannins (pink).

The resulting plots show that the values of all 20 occupational densities (D_1 – D_{20}) are very similar (within the standard deviations) for the isolates obtained by the two PPL-sorbents (FA_BE and the FA_BS isolates). At the same time, substantial differences can be seen between the SPE isolates and the parent FA. The SPE isolates contain the smaller portion of oxidized aromatic components of “hydrolysable tannins” chemotype (D_{13} , D_{17} – D_{18}) and lower portion of oxidized lipid- and terpenoid-like aliphatics (D_4 , D_5) along with the higher content of condensed tannins and lignin-like components (D_7 – D_8).

The obtained data allowed us a conclusion about identity of the molecular compositions of the SPE isolates obtained with a use of two different PPL sorbents—Bond ELut PPL and Bondesil PPL. The molecular compositions of both isolates deviate in the same way from molecular composition of the parent FA. For proving whether the same conclusions are supported by the data on structural group composition, we ran the NMR studies on the same set of samples.

3.3. NMR Results

Structural-group composition of the SPE isolates and the parent FA was determined with a use of ^{13}C and ^1H NMR analysis. The distribution of hydrogen and carbon atoms among the main structural fragments characteristic to HS was determined by integration

of the corresponding spectral regions. The assignments of spectral regions were made after [35]. The data obtained are shown in Figure 7.

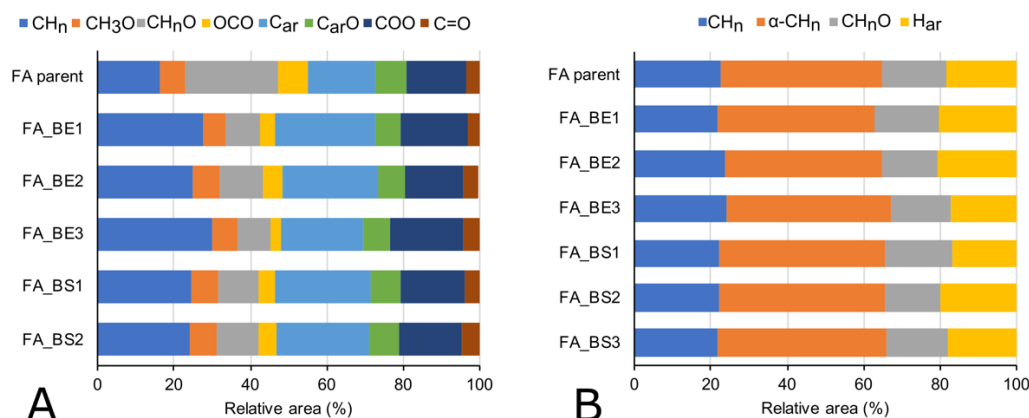


Figure 7. Distribution of integral intensities of C atoms (A) and H atoms (B) in the specified chemical environments (shown in the upper row of the Figure) in the parent FA and the FA isolates obtained with a use of the Bond Elut PPL sorbent (FA_BE) and Bondesil PPL sorbent (FA_BS). The data are measured by ^{13}C NMR (A) and ^1H NMR (B) spectroscopy.

Figure 7A shows the values of partial integrals of the eight common spectral regions in the ^{13}C NMR spectra of one FA sample and five SPE isolates used in this study. The data indicate substantial similarity among all five SPE isolates obtained with a use of Bond Elut PPL and Bondesil PPL sorbents. At the same time, the remarkable difference can be observed between the parent FA and the both FA-isolates with regard to the content of non-substituted aliphatic structures (CH_n), the content of carbohydrate carbon (CH_nO) and non-substituted aromatic carbon (C_{ar}). The parent FA is characterized with the higher content of hydrophilic carbohydrate carbon, whereas the FA isolates are enriched with more hydrophobic structures such as non-substituted aliphatic and aromatic groups. It should be noted that the above trends in structural-group compositions revealed by ^{13}C NMR spectroscopy for the samples used in this study are in very good agreement with the trends in molecular compositions revealed for the same samples by FT ICR MS. The obtained ^{13}C NMR data also corroborate well the reported values for FA [35,46–48].

The ^1H NMR spectra were obtained in D_2O and represented distribution of non-exchangeable protons in the samples used in this study (Figure 7B). The data demonstrate close similarity of all samples—including all SPE isolates and the parent FA—one to another. All spectra are characterized with prominent intensity of α -aliphatic region (1.6–3.1 ppm). The presence of lesser-substituted aromatic components and abundance in carbohydrates is a characteristic feature of FA according to the reported ^1H NMR data [49–51]. Distribution of non-exchangeable protons was much less characteristic of peculiar structural features of the parent FA versus its SPE isolates and did not reveal the differences, which could be clearly seen from the ^{13}C NMR data.

4. Conclusions

The results of comparative studies on sorption efficiency and molecular selectivity of two commercial sorbents—Bond Elut PPL and Bondesil PPL with regard to DOM components allow us to conclude on interchangeability of these two sorbents for the purposes of DOM isolation from natural waters. This conclusion is backed up by revealed very similar sorption behavior of the peat FA which was used as a model of DOM, on both sorbents and by high similarity of molecular compositions and carbon distribution among the main structural groups. The major difference between the sorbents was displayed in the lower extraction efficiency of the Bondesil PPL as compared to Bond Elut PPL. The maximum sorption efficiencies of the sorbents accounted for 60 and 75%, respectively. These differences could result from variation in the composition or morphology of the polymeric base of the both sorbents, nominally, from higher contribution of pore-filling

mechanism in case of Bond Elut PPL as compared to the Bondesil PPL sorbent. It could be also responsible for much more gradual decrease in sorption efficiency of Bond Elut PPL as compared to Bondesil PPL. At the same time, both sorbents yielded the same sorption affinity for molecular components of DOM. The slightly higher affinity of the both sorbents for more hydrophobic aromatics-enriched components of molecular ensemble of DOM was demonstrated by FT ICR MS. It is in sync with the apolar hydrophobic character of the sorbents. The revealed trend in molecular selectivity of both sorbents was supported by the data of ^{13}C NMR which demonstrated higher content of hydrophilic carbohydrate structures in the parent FA and less content of non-substituted aromatic and aliphatic groups as compared to those in the FA isolates derived with a use of both Bondesil PPL and Bond Elut PPL. In general, the conducted studies show good prospects for a use of bulk sorbent Bondesil PPL, which was newly applied in this study for the DOM isolation, for large-scale treatments aimed at gram-quantity isolation of DOM from natural waters.

Author Contributions: Conceptualization, I.V.P.; methodology, A.I.K., A.A.M., A.B.V.; data analysis, T.A.M., G.D.R.; investigation, A.N.K., A.A.M., S.V.M.; writing—original draft preparation, A.N.K.; writing—review and editing, I.V.P.; visualization, T.A.M., G.D.R., A.B.V. All authors have read and agreed to the published version of the manuscript.

Funding: This study was supported by the Russian Science Foundation: the grants 21-77-30001 (in part of the sorption studies) and 21-73-20202 (in part of the FT ICR MS studies). The research of I.V.P., A.I.K., and A.B.V. was partially supported by the State Contract 121021000105-7a “Molecular design, synthesis and study of physiologically active compounds, advancing the methodology of medicinal chemistry, chemoinformatics, and targeted chemical synthesis” (in part of NMR studies).

Institutional Review Board Statement: Not applicable.

Informed Consent Statement: Not applicable.

Data Availability Statement: Most data supporting the results are included in the article. The datasets used and/or analyzed during the current study are available from the corresponding author on reasonable request.

Acknowledgments: The financial support of the Russian Science Foundation is appreciated: grant # 21-73-20202 (FT ICR MS studies) and № 21-77-30001 (in part of the sorption studies). The research of I.V.P., A.I.K., and A.B.V. was partially supported by the State Contract 121021000105-7a “Molecular design, synthesis and study of physiologically active compounds, advancing the methodology of medicinal chemistry, chemoinformatics, and targeted chemical synthesis” (in part of NMR studies). The center of collective use of the Zelinsky IOC RAS is appreciated for availability of Solarix XR 15T (Bruker) FT ICR MS mass spectrometer. The interdisciplinary program of the Scientific Educational School of Lomonosov MSU “Future of the planet and global environmental change” is appreciated.

Conflicts of Interest: The authors declare no conflict of interest.

References

1. Baker, A.; Spencer, R.G. Characterization of dissolved organic matter from source to sea using fluorescence and absorbance spectroscopy. *Sci. Total Environ.* **2004**, *333*, 217–232. [\[CrossRef\]](#)
2. Meyers-Schulte, K.J.; Hedges, J.I. Molecular evidence for a terrestrial component of organic matter dissolved in ocean water. *Nat. Cell Biol.* **1986**, *321*, 61–63. [\[CrossRef\]](#)
3. Thurman, E.M. *Organic Geochemistry of Natural Waters*; Springer: Berlin, Germany, 1985.
4. Hertkorn, N.; Benner, R.; Frommberger, M.; Schmitt-Kopplin, P.; Witt, M.; Kaiser, K.; Kettrup, A.; Hedges, J.I. Characterization of a major refractory component of marine dissolved organic matter. *Geochim. Cosmochim. Acta* **2006**, *70*, 2990–3010. [\[CrossRef\]](#)
5. Xenopoulos, M.A.; Barnes, R.T.; Boodoo, K.S.; Butman, D.; Catalán, N.; D’Amario, S.C.; Fasching, C.; Kothawala, D.N.; Pisani, O.; Solomon, C.T.; et al. How humans alter dissolved organic matter composition in freshwater: Relevance for the Earth’s biogeochemistry. *Biogeochemistry* **2021**, *154*, 323–348. [\[CrossRef\]](#)
6. Green, N.; Perdue, E.M.; Aiken, G.R.; Butler, K.D.; Chen, H.; Dittmar, T.; Niggemann, J.; Stubbins, A. An intercomparison of three methods for the large-scale isolation of oceanic dissolved organic matter. *Mar. Chem.* **2014**, *161*, 14–19. [\[CrossRef\]](#)
7. Aiken, G.R.; Thurman, E.M.; Malcolm, R.L.; Walton, H.F. Comparison of XAD macroporous resins for the concentration of fulvic acid from aqueous solution. *Anal. Chem.* **1979**, *51*, 1799–1803. [\[CrossRef\]](#)

8. Thurman, E.M.; Malcolm, R.L.; Aiken, G.R. Prediction of capacity factors for aqueous organic solutes adsorbed on a porous acrylic resin. *Anal. Chem.* **1978**, *50*, 775–779. [[CrossRef](#)]
9. Daignault, S.; Noot, D.; Williams, D.; Huck, P. A review of the use of XAD resins to concentrate organic compounds in water. *Water Res.* **1988**, *22*, 803–813. [[CrossRef](#)]
10. Helms, J.R.; Mao, J.; Chen, H.; Perdue, E.M.; Green, N.W.; Hatcher, P.G.; Mopper, K.; Stubbins, A. Spectroscopic characterization of oceanic dissolved organic matter isolated by reverse osmosis coupled with electrodialysis. *Mar. Chem.* **2015**, *177*, 278–287. [[CrossRef](#)]
11. Tfaily, M.; Hodgkins, S.; Podgorski, D.C.; Chanton, J.P.; Cooper, W.T. Comparison of dialysis and solid-phase extraction for isolation and concentration of dissolved organic matter prior to Fourier transform ion cyclotron resonance mass spectrometry. *Anal. Bioanal. Chem.* **2012**, *404*, 447–457. [[CrossRef](#)]
12. Dittmar, T.; Koch, B.; Hertkorn, N.; Kattner, G. A simple and efficient method for the solid-phase extraction of dissolved organic matter (SPE-DOM) from seawater. *Limnol. Oceanogr. Methods* **2008**, *6*, 230–235. [[CrossRef](#)]
13. Swenson, M.M.; Oyler, A.R.; Minor, E. Rapid solid phase extraction of dissolved organic matter. *Limnol. Oceanogr. Methods* **2014**, *12*, 713–728. [[CrossRef](#)]
14. Zherebker, A.Y.; Perminova, I.V.; Kononikhin, A.I.; Volikov, A.B.; Kostyukevich, Y.I.; Kononikhin, A.S.; Nikolaev, E.N. Extraction of humic substances from fresh waters on solid-phase cartridges and their study by Fourier transform ion cyclotron resonance mass spectrometry. *J. Anal. Chem.* **2016**, *71*, 372–378. [[CrossRef](#)]
15. Minor, E.C.; Swenson, M.M.; Mattson, B.M.; Oyler, A.R. Structural characterization of dissolved organic matter: A review of current techniques for isolation and analysis. *Environ. Sci. Process. Impacts* **2014**, *16*, 2064–2079. [[CrossRef](#)]
16. Li, Y.; Harir, M.; Lucio, M.; Kanawati, B.; Smirnov, K.; Flerus, R.; Koch, B.; Schmitt-Kopplin, P.; Hertkorn, N. Proposed guidelines for solid phase extraction of Suwannee River dissolved organic matter. *Anal. Chem.* **2016**, *88*, 6680–6688. [[CrossRef](#)] [[PubMed](#)]
17. Arellano, A.R.; Bianchi, T.S.; Hutchings, J.; Shields, M.R.; Cui, X. Differential effects of solid-phase extraction resins on the measurement of dissolved lignin-phenols and organic matter composition in natural waters. *Limnol. Oceanogr. Methods* **2018**, *16*, 22–34. [[CrossRef](#)]
18. Perminova, I.V.; Dubinenkov, I.V.; Kononikhin, A.S.; Konstantinov, A.I.; Zherebker, A.Y.; Andzhushev, M.A.; Lebedev, V.A.; Bulygina, E.; Holmes, R.M.; Kostyukevich, Y.I.; et al. Molecular mapping of sorbent selectivities with respect to isolation of arctic dissolved organic matter as measured by Fourier transform mass spectrometry. *Environ. Sci. Technol.* **2014**, *48*, 7461–7468. [[CrossRef](#)]
19. Sleighter, R.L.; Hatcher, P.G. Molecular characterization of dissolved organic matter (DOM) along a river to ocean transect of the lower Chesapeake Bay by ultrahigh resolution electrospray ionization Fourier transform ion cyclotron resonance mass spectrometry. *Mar. Chem.* **2008**, *110*, 140–152. [[CrossRef](#)]
20. D’Auria, M.; Emanuele, L.; Racioppi, R. A FT-ICR MS study of Lignin: Determination of an unusual structural repetitive unit in steam exploded lignin from Wheat Straw. *Lett. Org. Chem.* **2011**, *8*, 436–446. [[CrossRef](#)]
21. Ning, C.; Gao, Y.; Yu, H.; Zhang, H.; Geng, N.; Cao, R.; Chen, J. FT-ICR mass spectrometry for molecular characterization of water-insoluble organic compounds in winter atmospheric fine particulate matters. *J. Environ. Sci.* **2022**, *111*, 51–60. [[CrossRef](#)]
22. Hertkorn, N.; Harir, M.; Koch, B.P.; Michalke, B.; Schmitt-Kopplin, P. High-field NMR spectroscopy and FTICR mass spectrometry: Powerful discovery tools for the molecular level characterization of marine dissolved organic matter. *Biogeosciences* **2013**, *10*, 1583–1624. [[CrossRef](#)]
23. Qi, Y.; Fu, P.; Volmer, D.A. Analysis of natural organic matter via Fourier transform ion cyclotron resonance mass spectrometry: An overview of recent non-petroleum applications. *Mass Spectrom. Rev.* **2020**, *00*, 1–15. [[CrossRef](#)]
24. Hertkorn, N.; Ruecker, C.; Meringer, M.; Gugisch, R.; Frommberger, M.; Perdue, E.M.; Witt, M.; Schmitt-Kopplin, P. High-precision frequency measurements: Indispensable tools at the core of the molecular-level analysis of complex systems. *Anal. Bioanal. Chem.* **2007**, *389*, 1311–1327. [[CrossRef](#)] [[PubMed](#)]
25. Derrien, M.; Lee, Y.K.; Park, J.-E.; Li, P.; Chen, M.; Lee, S.H.; Lee, S.H.; Lee, J.-B.; Hur, J. Spectroscopic and molecular characterization of humic substances (HS) from soils and sediments in a watershed: Comparative study of HS chemical fractions and the origins. *Environ. Sci. Pollut. Res.* **2017**, *24*, 16933–16945. [[CrossRef](#)]
26. Simpson, A.J.; Brown, S.A. Purge NMR: Effective and easy solvent suppression. *J. Magn. Reson.* **2005**, *175*, 340–346. [[CrossRef](#)]
27. Simpson, A.J.; McNally, D.J.; Simpson, M. NMR spectroscopy in environmental research: From molecular interactions to global processes. *Prog. Nucl. Magn. Reson. Spectrosc.* **2011**, *58*, 97–175. [[CrossRef](#)]
28. Hertkorn, N.; Kettrup, A. Molecular level structural analysis of natural organic matter and of humic substances by multinuclear and higher dimensional NMR spectroscopy. In *Use of Humic Substances to Remediate Polluted Environments: From Theory to Practice*; Perminova, I.V., Hatfield, K., Hertkorn, N., Eds.; Springer: Dordrecht, The Netherlands, 2005; pp. 391–435.
29. Mopper, K.; Stubbins, A.; Ritchie, J.D.; Bialk, H.M.; Hatcher, P.G. Advanced instrumental approaches for characterization of marine dissolved organic matter: Extraction techniques, mass spectrometry, and nuclear magnetic resonance spectroscopy. *Chem. Rev.* **2007**, *107*, 419–442. [[CrossRef](#)] [[PubMed](#)]
30. Schmitt-Kopplin, P.; Gelencsér, A.; Dabek-Zlotorzynska, E.; Kiss, G.; Hertkorn, N.; Harir, M.; Hong, Y.; Gebefügi, I. Analysis of the unresolved organic fraction in atmospheric aerosols with ultrahigh-resolution mass spectrometry and nuclear magnetic resonance spectroscopy: Organosulfates as photochemical smog constituents. *Anal. Chem.* **2010**, *82*, 8017–8026. [[CrossRef](#)]

31. Mueller, C.; Kremb, S.; Gonsior, M.; Brack-Werner, R.; Voolstra, C.R.; Schmitt-Kopplin, P. Advanced identification of global bioactivity hotspots via screening of the metabolic fingerprint of entire ecosystems. *Sci. Rep.* **2020**, *10*, 1–13. [[CrossRef](#)]
32. Schmitt-Kopplin, P.; Gabelica, Z.; Gougeon, R.; Fekete, A.; Kanawati, B.; Harir, M.; Gebefuegi, I.; Eckel, G.; Hertkorn, N. High molecular diversity of extraterrestrial organic matter in Murchison meteorite revealed 40 years after its fall. *Proc. Natl. Acad. Sci. USA* **2010**, *107*, 2763–2768. [[CrossRef](#)]
33. Kruger, B.R.; Dalzell, B.J.; Minor, E.C. Effect of organic matter source and salinity on dissolved organic matter isolation via ultrafiltration and solid phase extraction. *Aquat. Sci.* **2011**, *73*, 405–417. [[CrossRef](#)]
34. Kovalevskii, D.V.; Permin, A.B.; Perminova, I.V.; Petrosyan, V.S. Conditions for acquiring quantitative ¹³C NMR spectra of humic substances. *Mosc. State Univ. Bull.* **2000**, *41*, 39–42.
35. Hertkorn, N.; Permin, A.; Perminova, I.; Kovalevskii, D.; Yudov, M.; Petrosyan, V.; Kettrup, A. Comparative analysis of partial structures of a peat humic and fulvic acid using one- and two-dimensional nuclear magnetic resonance spectroscopy. *J. Environ. Qual.* **2002**, *31*, 375–387. [[CrossRef](#)]
36. Koch, B.P.; Dittmar, T.; Witt, M.; Kattner, G. Fundamentals of molecular formula assignment to ultrahigh resolution mass data of natural organic matter. *Anal. Chem.* **2007**, *79*, 1758–1763. [[CrossRef](#)] [[PubMed](#)]
37. Kunenkov, E.V.; Kononikhin, A.S.; Perminova, I.V.; Hertkorn, N.; Gaspar, A.; Schmitt-Kopplin, P.; Popov, I.A.; Garmash, A.V.; Nikolaev, E.N. Total mass difference statistics algorithm: A new approach to identification of high-mass building blocks in electrospray ionization Fourier transform ion cyclotron mass spectrometry data of natural organic matter. *Anal. Chem.* **2009**, *81*, 10106–10115. [[CrossRef](#)] [[PubMed](#)]
38. Kim, S.; Simpson, A.J.; Kujawinski, E.B.; Freitas, M.A.; Hatcher, P.G. High resolution electrospray ionization mass spectrometry and 2D solution NMR for the analysis of DOM extracted by C18 solid phase disk. *Org. Geochem.* **2003**, *34*, 1325–1335. [[CrossRef](#)]
39. Zhrebker, A.; Kim, S.; Schmitt-Kopplin, P.; Spencer, R.G.M.; Lechtenfeld, O.; Podgorski, D.C.; Hertkorn, N.; Harir, M.; Nurfajin, N.; Koch, B.; et al. Interlaboratory comparison of humic substances compositional space as measured by Fourier transform ion cyclotron resonance mass spectrometry (IUPAC Technical Report). *Pure Appl. Chem.* **2020**, *92*, 1447–1467. [[CrossRef](#)]
40. Fligner, A.M.; Verducci, J.S.; Blower, E.P. A modification of the Jaccard–Tanimoto Similarity index for diverse selection of chemical compounds using binary strings. *Technometrics* **2002**, *44*, 110–119. [[CrossRef](#)]
41. Bajusz, D.; RÁCZ, A.; Héberger, K. Why is Tanimoto index an appropriate choice for fingerprint-based similarity calculations? *J. Cheminform.* **2015**, *7*, 1–13. [[CrossRef](#)]
42. Perminova, I.V. From green chemistry and nature-like technologies towards ecoadaptive chemistry and technology. *Pure Appl. Chem.* **2019**, *91*, 851–864. [[CrossRef](#)]
43. Kujawinski, E.B.; Behn, M.D. Automated analysis of electrospray ionization Fourier transform ion cyclotron resonance mass spectra of natural organic matter. *Anal. Chem.* **2006**, *78*, 4363–4373. [[CrossRef](#)] [[PubMed](#)]
44. Thurman, E.M.; Mills, M.S. *Solid-Phase Extraction: Principles and Practice*; Wiley: New York, NY, USA, 1998.
45. Mosher, J.J.; Klein, G.C.; Marshall, A.G.; Findlay, R.H. Influence of bedrock geology on dissolved organic matter quality in stream water. *Org. Geochem.* **2010**, *41*, 1177–1188. [[CrossRef](#)]
46. Lodygin, E.D.; Beznosikov, V.A. The ¹³C NMR study of the molecular structure of humus acids from podzolic and bog-podzolic soils. *Eurasian Soil Sci.* **2003**, *36*, 967–975.
47. Kholodov, V.A.; Konstantinov, A.I.; Kudryavtsev, A.V.; Perminova, I.V. Structure of humic acids in zonal soils from ¹³C NMR data. *Eurasian Soil Sci.* **2011**, *44*, 976–983. [[CrossRef](#)]
48. Einsiedl, F.; Hertkorn, N.; Wolf, M.; Frommberger, M.; Schmitt-Kopplin, P.; Koch, B.P. Rapid biotic molecular transformation of fulvic acids in a karst aquifer. *Geochim. Cosmochim. Acta* **2007**, *71*, 5474–5482. [[CrossRef](#)]
49. Ruggiero, P.; Interesse, F.S.; Cassidei, L.; Sciacovelli, O. ¹H NMR spectra of humic and fulvic acids and their peracetic oxidation products. *Geochim. Cosmochim. Acta* **1980**, *44*, 603–609. [[CrossRef](#)]
50. Machado, W.; Franchini, J.C.; Guimarães, M.D.F.; Filho, J.T. Spectroscopic characterization of humic and fulvic acids in soil aggregates, Brazil. *Heliyon* **2020**, *6*, e04078. [[CrossRef](#)]
51. Rodríguez, F.J.; Schlenger, P.; García-Valverde, M. Monitoring changes in the structure and properties of humic substances following ozonation using UV–Vis, FTIR and ¹H NMR techniques. *Sci. Total Environ.* **2016**, *541*, 623–637. [[CrossRef](#)]